Recent Advances in Niobium-Based Coatings: Properties, Characteristics, and Applications

Kamlesh V. Chauhan[1], Sushant Rawal[2,*] and Vandan Vyas[3], Noor M. Mohammad[4] and Anil FNU5,

[1]*CHAMOS Matrusanstha Department of Mechanical Engineering, Chandubhai S. Patel Institute of Technology (CSPIT), Charotar University of Science and Technology (CHARUSAT), Changa-388421, Gujarat, India*

[2]*McMaster Manufacturing Research Institute (MMRI), Department of Mechanical Engineering, McMaster University, 1280 Main Street West, Hamilton, ON L8S4L7, Canada*

[3]*L J Institute of Engineering and Technology, LJ University, LJ Campus, Near Sarkhej-Sanand Circle, Off S.G. Road, Makarba, Ahmedabad, Gujarat – 382210, India*

[4]*School of Mechanical Engineering, Purdue University, West Lafayette, 47907, IN, USA*

[5]*Ira A. Fulton Schools of Engineering, Arizona State University, Tempe, AZ 85281, USA*

Abstract: Transition metals exhibit unique characteristics such as high melting points and boiling points, making them valuable for thin film technology. Since the 1960s, these properties have supported decorative coatings, cutting tool hard coatings, optical coatings, and protective coatings. Among transition metals, niobium thin films serve waveguides, electrochromic devices, oxygen sensors, semiconductors, and medical implants. Researchers have investigated structural, mechanical, optical, and tribological properties of niobium and its alloy thin films extensively. Studied parameters include hardness, refractive index, grain size, thickness, wear resistance, and friction coefficient for specific applications. Common deposition techniques include DC/RF magnetron sputtering, sol-gel coating, spray pyrolysis, and physical vapor deposition. Unlike prior reviews focused on single niobium compounds, this article compares three niobium-based coatings across all major properties. This review summarizes structural, optical, electrical, mechanical, and tribological properties of niobium oxide, niobium nitride, and niobium carbide coatings.

Keywords: Hardness, Nb_2O_5, NbN, NbC, PVD, Surface Roughness, Thin Film.

1. INTRODUCTION

Niobium is a shiny, silver metal that crystallizes in a body-centred cubic (BCC) lattice structure. Its melting point and boiling point are 2477°C and 4744°C, with a density of 8.57 g/cm³ [1]. At 27.3 K, below its critical temperature, niobium shows an electrical resistivity of 15.2 μΩ·cm [1]. Niobium forms stable oxides, nitrides, carbides, and oxy-nitrides through high interatomic bonding energies [2]. Niobium and its alloys show high corrosion resistance across several different environmental conditions [3, 4]. Their high ductility and low density at room temperature support fabrication of complex structures [4].

Niobium is commonly added to nickel-based turbines for power generation and nickel-based superalloys for aircraft engines [4]. It also shows strong potential for biomedical devices and implants, being biocompatible like zirconium [5]. Niobium coatings offer good mechanical properties for dental implants, which face repeated loads and fatigue cycles [6]. These coatings combine metallic strength with good corrosion resistance under such demanding conditions [6]. Niobium also serves oxygen sensors, solar control devices, and electrochromic films in current applications [7]. Niobium thin films function in cryogenic devices, diffusion barriers in Josephson junctions, and superconducting cable coatings [6]. Film hardness, refractive index, corrosion resistance, coloration efficiency, band gap, and compressive stress all depend on deposition parameters. Recent aircraft engine and biomedical applications show niobium hardness comparable to titanium and zirconium alloys [8].

Several reviews have already examined niobium and its alloys as general thin film coating materials.

*Address correspondence to this author at McMaster Manufacturing Research Institute (MMRI), Department of Mechanical Engineering, McMaster University, 1280 Main Street West, Hamilton, ON L8S4L7, Canada;
E-mail: sushant@mcmaster.ca

Received on 11-06-2026 Accepted on 05-08-2026 Published on 13-08-2026

E-ISSN: 3110-9772/26

However, few reviews compare niobium oxide, niobium nitride, and niobium carbide coatings directly against each other. This review addresses that gap by comparing structural, mechanical, optical, electrical, and tribological properties across all three materials. It also links deposition parameters to resulting microstructure and functional properties in a dedicated comparative section, presented later in this review.

Figure **1** maps this scope directly: the three coating families along one axis, the five compared property classes along a second, and the application domains they feed into along a third, framing the structure the rest of the review follows.

2. NIOBIUM OXIDE COATINGS

Niobium oxide is a general term covering niobium monoxide, niobium dioxide, and niobium pentoxide, the most stable form [9].

Nb_2O_5 coatings support osteoblast adhesion for biomedical implants and solid electrolytic capacitor construction.[9], [10] Niobium films also serve quantum bit fabrication and single-photon detector applications in recent research [11]. These compounds range from optical waveguides and capacitor dielectrics to oxygen sensors and corrosion-resistant coatings [12, 13]. NbO films additionally function as refractive-index layers within multilayer optical interference filter stacks [14]. Niobium oxide is also a constituent of lithium niobate, barium, and lead compound oxides used in modulators [15, 16]. The material shows excellent chemical and thermal stability across a wide range of operating conditions [17].

2.1. Niobium Pentoxide as a High-Permittivity Dielectric

Niobium pentoxide, the most stable oxide form, attracts strong interest as a high-permittivity gate dielectric. Over the last two decades, its stable form and chemical durability have driven emerging electronic applications. Niobium pentoxide is now used in non-aqueous lithium battery electrodes, electrochromic devices, and catalysis [18]. Nanocrystalline solar cell electrodes also benefit from niobium pentoxide's stability and favourable electrochemical behaviour [19].

2.2. Deposition by Magnetron Sputtering

Magnetron sputtering is the dominant deposition route reported for Nb_2O_5 coatings in the reviewed literature [20, 21]. Increasing annealing temperature from 100 to 600°C decreases sputtered film thickness while increasing surface roughness [20]. Sputtering pressure and RF power jointly govern the refractive index and thickness of RF-sputtered films [22]. Reactive RF sputtering with post-deposition heat treatment increases surface roughness while stabilising the optical band gap [23]. Substrate bias between 0 and −200 V tunes both band gap and hardness of bias-sputtered films [24]. You, Jiang, Cao, and colleagues showed target power between 450 and 900 W tunes

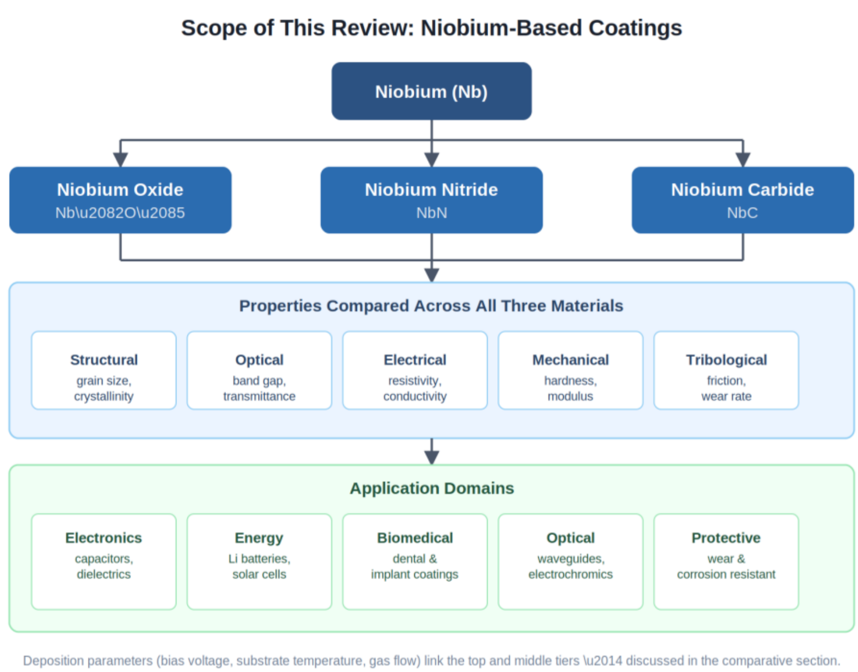

Figure 1: Scope of the review: niobium-based coating materials, compared properties, and application domains.

deposition rate and composition [25]. RF sputtering power and substrate temperature jointly determine thickness in antireflection-grade Nb_2O_5 coatings.[26] Reactive DC sputtering with controlled oxygen flow yields films with band gap near 3.4 eV [27]. Lee, Liu, Malhado, and colleagues showed broad-beam ion-source sputtering triples deposition rate over conventional methods [28]. Across these sputtering studies, hardness values cluster between 5 and 11 GPa depending on deposition energy [24, 29].

2.3. Deposition by Sol-Gel, Spin Coating, and Spray Pyrolysis

Sol-gel dip coating produces Nb_2O_5 films with a wider optical band gap than sputtered equivalents.[30] Salim, Shafeeq, AbdulRazzaq, and colleagues showed substrate temperature between 250 and 650°C shifts band gap in pulsed-laser-deposited films [31]. Post-annealing treatment after spray pyrolysis significantly increases both surface roughness and grain size [32]. These solution- and laser-based routes generally require lower capital equipment cost than vacuum sputtering methods [31].

2.4. Deposition by Atomic Layer Deposition, with Recent Optical Characterization

Atomic layer deposition produces the thinnest reported Nb_2O_5 films, around 1.5 nanometres in thickness [17]. Franta, Hroncová, Dvořák, and colleagues combined ellipsometry and spectrophotometry across five film thicknesses in 2024 [33]. Their universal dispersion model determined optical constants across an unprecedented spectral range [33]. This directly strengthens the optical-property dataset available across all deposition techniques [33].

Valente *et al*. examined niobium film properties as a function of deposition energy in detail.[34] Sapphire-substrate films show good crystal orientation with a very sharp film-substrate interface [34]. Cross-section transmission electron micrographs confirm epitaxial growth of niobium on sapphire [34]. Increasing substrate bias voltage from −60 V to −90 V visibly coarsens the resulting grain structure [34].

Together, Figs. (**2** and **3**) show that substrate bias governs grain coarsening independently of the underlying substrate — sapphire and copper both show visibly coarser grains at −90 V than at −60/−90 V comparisons in the copper case — reinforcing deposition energy as the cross-material controlling variable identified later in Table **4**.

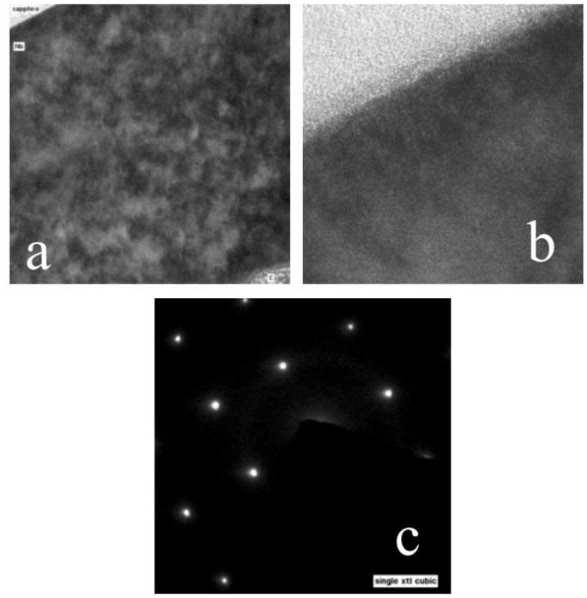

Figure 2: Niobium film on sapphire deposited at −90V substrate bias: cross-section TEM view (a), cross-section view of the niobium–sapphire surface (b), and electron diffraction pattern showing (100) crystal orientation (c) [34].

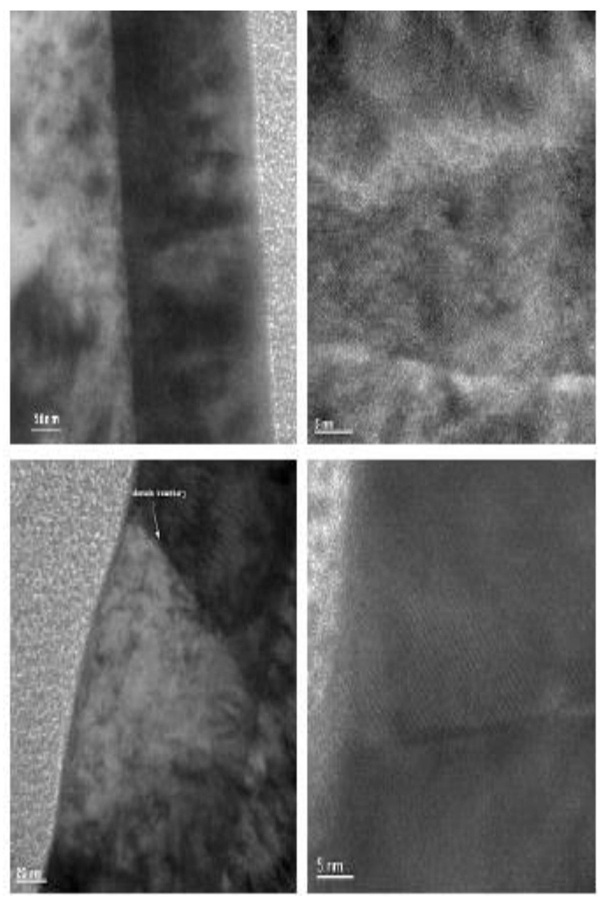

Figure 3: Cross-section TEM micrographs of niobium film on copper deposited at −60V (top) and −90V (bottom) substrate bias, showing bias-dependent grain coarsening [34].

2.5. Recent Biomedical Coating Application

da Silva, Baptista, Albuquerque, and colleagues examined Nb_2O_5-coated Ti-6Al-4V alloy for dental implants in 2026 [35]. Coated surfaces retained substantially less organic material than uncoated surfaces after artificial saliva exposure [35]. The coating also reduced Escherichia coli biofilm coverage from 74.94% down to 51.10% [35]. This directly addresses the previously identified gap in Nb_2O_5 wettability and biomedical property data [35].

2.6. Review of Niobium Pentoxide Thin Films

Table **1** condenses the deposition-technique groupings above into a single comparative reference. Read across entries, sputtering-based routes account for the majority of reported studies and cluster around band gaps of 3.4–3.6 eV and hardness values of 5–11 GPa, while the single ALD entry produces markedly thinner films (1.5 nm) with roughness below 0.1 nm — an order of magnitude smoother than any sputtered or solution-processed film in the table. Sol-gel and spray-pyrolysis entries show the widest band-gap scatter (2.8–5.3 eV), consistent with their lower process control relative to vacuum-based methods.

3. NIOBIUM NITRIDE (NbN) COATINGS

Niobium nitride remains a strong candidate material for cryogenic radiation detectors and superconducting electronic devices [41]. Their relatively high critical superconducting temperature allows use as diffusion barriers in Josephson junctions [23]. Transition-metal nitrides incorporating both nitrogen and oxygen atoms display distinctive combined properties [42]. Researchers remain interested in NbN's corrosion resistance, high melting point, and biocompatibility for

Table 1: Review of niobium pentoxide thin films.

Research Group	Deposition Technique	Substrate	Parameters Studied	Properties Examined
Li, Cao, *et al*. (2016) [36]	DC magnetron sputtering	Si	Deposition & base pressure	Thickness 4.71–22.8 nm; hardness 5.39 GPa
Venkataraj, Drese, *et al*. (2001) [15]	DC magnetron sputtering	Glass, Si	Cathode current; O_2 flow (0–30 sccm)	Band gap 3.5–3.6 eV; density 4.09 g/cm³; thickness 200–217 nm
Coşkun & Demirela (2013) [20]	RF magnetron sputtering	Glass	Sputtering pressure (3–15 mTorr)	Refractive index 2.00–2.32; thickness 168–415 nm
Coşkun, Demirel, Atak (2015) [37]	RF magnetron sputtering (heat-treated)	Glass	Pressure (2×10^{-4} Torr); RF power 75 W; 300°C	Band gap 3.65 eV; thickness 377 nm; roughness 1.13–3.98 nm
Zaitsev *et al*. (2010) [29]	Reactive RF sputtering	Quartz wafer	O_2 pressure (19.5 Pa); sputter pressure	Thickness 87–401 nm; deposition rate 7.4 nm/min
Rani, Zoolfakar, *et al*. [21]	Reactive sputtering (bias-dependent)	Glass	Substrate bias (0 to −200 V); target power (300 W)	Band gap 3.1–5.3 eV; refractive index 2–2.3; hardness 5.6–6.8 GPa
Al-Baradi *et al*. (2018) [22]	RF magnetron sputtering	Glass	RF power (150–200 W); substrate temp. 300 K	Band gap 3.79–3.84 eV; thickness 950–1094 nm
Miki *et al*. (1996) [38]	Reactive DC magnetron sputtering	Glass	Chamber & total pressure; O_2 flow (10 sccm)	Band gap 3.41 eV; transmittance 80%; thickness 500 nm
Romero, Leinen, *et al*. (2004) [39]	Spray pyrolysis	Glass, silica	Spray solution ratio; substrate temp. (380–500°C)	Thickness 280 nm
Mujawar *et al*. (2007) [40]	Spray pyrolysis (post-annealed)	Glass	Substrate temperature (500°C)	Band gap 2.8–3.8 eV; roughness 24–299 nm; grain 4–10 µm
Huang, Xu, *et al*. (2011) [17]	Atomic layer deposition	Si(100)	Working pressure; substrate temp. (300°C)	Thickness 1.5 nm; roughness 0.098–1.52 nm
Salim, Shafeeq, Abdul-Razzaq, *et al*. (2023) [31]	Pulsed laser deposition (Nd:YAG)	Not specified	Substrate temperature (250–650°C)	Polycrystalline phases; band gap shifts with temperature
You, Jiang, Cao, *et al*. (2023) [25]	Ion-assisted reactive magnetron sputtering	Si	Target power (450–900 W)	Deposition rate 0.88–2.05 Å/s; tunable $Nb_2O_5 \leftrightarrow NbO_2$
Lee, Liu, Malhado, *et al*. (2025) [28]	MetaMode broad-beam ion source sputtering	Glass, Si	O_2 concentration (7.5–20%)	3× higher deposition rate; smoother, denser films
Franta, Hroncová, Dvořák, *et al*. (2024) [33]	N/A (optical characterization)	5 samples, various	Film thickness (20–250 nm)	Wide-spectral-range optical constants via dispersion model
da Silva, Baptista, *et al*. (2026) [35]	Reactive DC sputtering	Ti-6Al-4V alloy	Coating presence (coated vs. uncoated)	Reduced salivary retention and bacterial biofilm coverage

varied applications [30, 43, 44]. Recent work extends these applications toward fuel-cell bipolar plates and biomedical implant coatings [24, 45].

3.1. Deposition by Reactive DC/RF Magnetron Sputtering

Reactive magnetron sputtering is the dominant deposition route reported for NbN coatings in the reviewed literature [24, 45-50]. Borowski *et al*. deposited NbN on AISI 316L steel using reactive DC magnetron sputtering; increasing the post-deposition air-oxidation temperature raised microhardness and corrosion resistance while forming an orthorhombic Nb_2O_5 surface layer [45]. Mahmood, Chaker, Khalaf, and Chaker showed sputtering power (80–160 W) and substrate temperature (40–200°C) jointly determine grain size and crystallinity in RF-sputtered NbN on medical-grade Ti6Al4V alloy [24]. Abdallah, Kakhia, Masloub, and Zetoune found sputtering power (100–150 W) directly governs crystallinity, corrosion resistance, and microhardness in DC-sputtered NbN on stainless steel and silicon.[46] Dahal, Gu, Su, and Wang showed increasing sputtering power shifts preferred crystal orientation from single-phase (111) toward mixed (111)/(200).[47] Pei, Fan, Ni, and Gu demonstrated that annealing at 900°C after DC magnetron sputtering reduces film stress while increasing grain size and crystallinity, with superconducting critical temperature and resistivity tied to the N/Nb ratio [48]. Stepanov, Baburin, Kushnev, and colleagues mapped sputtering recipe against superconducting Tc (2.5–12.1 K) and sheet resistance (285–2000 Ω/sq) across more than 100 depositions [49]. Tolpygo, Mallek, Bolkhovsky, and colleagues compared reactive sputtering with PECVD, reporting Tc of 9–15.5 K and kinetic inductance of 3 pH/sq relevant to via and interconnect performance [50]. Guo, Wang, Fang, Zhang, Sun, and Wan extended this deposition route to tribological performance, showing sputtered NbN reduces wear rate by 97.5% relative to uncoated steel under oil lubrication via a self-forming Nb_2O_5 lubricating film [51]. Across these studies, sputtering power and nitrogen partial pressure emerge as the two parameters with the most direct influence on both crystallographic phase and downstream mechanical or superconducting performance.

3.2. Deposition by High-Energy Routes: Arc Ion Plating, Cathodic-Arc Evaporation, and HiPIMS

High-energy deposition routes produce the highest hardness values reported for NbN coatings. Fu, Li, Chen, Guo, and Wang used arc ion plating to deposit NbN and NbN-Ag nanocomposite films, reaching hardness values up to 44 GPa with strong adhesion in pure NbN; silver doping reduced the friction coefficient but degraded wear resistance overall [52]. Smyrnova, Sahul, Haršáni, and colleagues used cathodic-arc evaporation to deposit WN/NbN multilayer coatings on steel, showing negative bias voltage (50–200 V) tunes hardness between 33.6 and 36.6 GPa and wear rate between 1.9 and 4.1 $\times 10^{-6}$ mm^3/Nm [53]. Horne, Hugo, Reid, and Santavicca compared reactive DC sputtering against HiPIMS for NbN on oxidized silicon, finding HiPIMS yields higher superconducting Tc than conventional DC sputtering at matched nitrogen concentration and film thickness [27]. Johar, Shahgaldi, and colleagues combined magnetron sputtering with a TiN interlayer to deposit NbN and TaN on titanium bipolar plates; both coatings suppressed titanium's native passivation layer and improved conductivity and corrosion resistance, a new application area for high-energy-route NbN coatings [54]. Figure (**4**) illustrates wear-track morphology for a magnetron-sputtered NbN_x coating at 40% nitrogen partial pressure. The narrow, shallow track and limited debris consistent with this micrograph corroborate the low wear rates reported for high-energy NbN routes above, and visually link the nitrogen-partial-pressure control variable to the tribological outcome quantified in Table **2** [55].

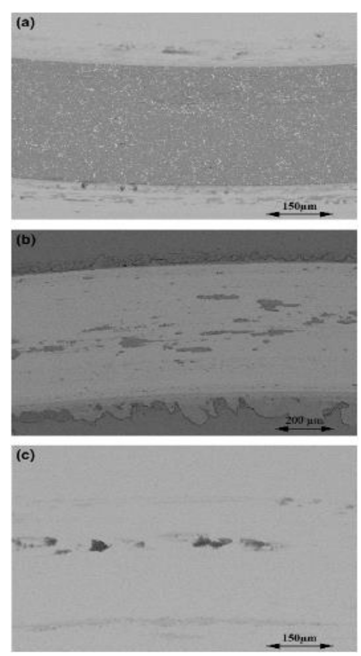

Figure 4: Scanning electron micrographs of wear tracks formed during tribotesting of NbN_x coating deposited at 40% nitrogen partial pressure against an alumina ball, now supported by comparable recent hardness and friction data [55].

3.3. Deposition by Atomic Layer Deposition and PECVD

Atomic layer deposition and its plasma-enhanced variant increasingly target wafer-scale uniformity for quantum and superconducting device integration. Lennon, Shu, Brennan, and colleagues used plasma-enhanced ALD to grow NbN on 200 mm silicon wafers, achieving superconducting Tc up to 13.5 K with sheet-resistance variation below 7% across the wafer, a uniformity not reported for sputtered films [26]. Wang, Wu, Pieczulewski, and colleagues extended ALD to a full NbN/AlN/NbN Josephson-junction stack on a qubit chip, showing AlN barrier thickness, set by ALD cycle count, tunes critical current density [23]. Together, these studies position ALD/PEALD as the emerging route of choice where wafer-scale reproducibility outweighs the higher hardness achievable by high-energy PVD methods.

3.4. Other Deposition Routes: MOCVD, CVD, and Multilayer Architectures

Earlier deposition routes remain relevant as points of comparison. Bekermann, Barreca, and colleagues used MOCVD to grow niobium nitride and oxynitride films, establishing growth-condition/composition relationships that predate the sputtering-dominated recent literature [30]. Fenker, Kappl, Banakh, Martin, and Pierson used reactive magnetron sputtering to deposit niobium oxynitride specifically, showing that nitrogen–oxygen co-incorporation produces compositional behavior distinct from either pure nitride or pure oxide films [44]. Savisalo, Lewis, and Hovsepian deposited CrON/NbON nano-scale multilayers, showing layer periodicity governs wear and corrosion resistance in multilayer architectures [43]. Manaud, Poulon, Gomez, and Petitcorps compared NbN against CrN, ZrN, and TaN as CVD diffusion barriers on WC–Co cutting tools, providing one of the few direct inter-nitride comparative datasets available for this material class [56]. Graça, Holz, Loureiro, Mather, and Fagg used ammonolysis of Nb_2O_5 powder to control oxynitride phase and oxidation kinetics, a non-vacuum route distinct from the sputtering and ALD methods above [42]. Cucciniello and colleagues' 2022 review of sputtering, ALD, and CVD growth routes for NbN provides the processing–structure–property framework this section builds on [41]. Kern and colleagues' spectroscopic ellipsometry study of ultrathin disordered NbN films is a characterization rather than deposition study, but resolves electron relaxation rate, Fermi velocity, and density-of-states parameters relevant to interpreting the electrical properties reported across the deposition routes above [57].

Table **2** compiles these NbN studies for direct comparison. The spread is wider than for Nb_2O_5: reactive magnetron sputtering delivers moderate hardness and the broadest range of reported superconducting Tc (2.5–15.5 K depending on recipe), while high-energy routes — arc ion plating and cathodic-arc evaporation — push hardness to 33–44 GPa at the cost of stoichiometric precision. PEALD is the outlier in reproducibility, holding sheet-resistance variation below 7% across a 200 mm wafer, a uniformity no sputtered entry in the table matches.

4. NIOBIUM CARBIDE (NBC) COATINGS

4.1. Deposition by Sintering and Diffusion-Based Routes

Li, Bai, and colleagues fabricated niobium carbide coatings on GCr15 bearing steel using in-situ hot press sintering, achieving superhardness of 20.2 GPa with interfacial bond strength above 210 MPa; grain morphology graded from equiaxed Nb_2C near the substrate to columnar and then equiaxed NbC near the surface, driven by a carbon-concentration diffusion gradient [58]. Khmelnitsky and colleagues used niobium deposition followed by vacuum annealing of diamond substrates, showing niobium converts to Nb_2C after annealing and then to NbC above 1200°C, with the resulting few-nanometre-thick NbC film reaching superconducting Tc up to 12.4 K, among the highest reported for carbide phases.[59] Across both diffusion-based routes, anneal or sintering temperature is the parameter that most directly controls the Nb_2C-to-NbC phase transition and the resulting hardness or superconducting response.

4.2. Deposition by Physical Vapor Deposition (HiPIMS)

Bahr and colleagues used non-reactive HiPIMS to deposit NbC_x films across a target peak power density range of 0.11–1.48 kW/cm²; increasing power density reduced the C/Nb ratio from 1.52 to 0.99, shifting film microstructure from nanocomposite toward columnar grain structure, with lower C/Nb ratios producing denser, harder films [60]. This establishes HiPIMS peak power density as the primary lever controlling NbC stoichiometry and hardness, a role comparable to sputtering power in the NbN literature above.

Table 2: Review of niobium nitride thin films.

Research Group	Deposition Technique	Substrate	Parameters Studied	Properties Examined
Borowski *et al*. (2023) [45]	Reactive DC magnetron sputtering	AISI 316L steel	Air oxidation temperature; sputtering time	Ca/P ratio near hydroxyapatite; increased microhardness; hydrophilic surface
Mahmood, Chaker, Khalaf, Chaker (2024) [24]	RF magnetron sputtering	Ti6Al4V alloy	Power (80–160 W); substrate temp. (40–200°C)	Cubic polycrystalline structure; grain size varies with power/temperature
Johar, Shahgaldi, *et al*. (2026) [54]	Magnetron sputtering + TiN interlayer	Titanium (bipolar plate)	Coating composition (NbN vs. TaN)	Suppressed passivation; improved conductivity and corrosion resistance
Dahal, Gu, Su, Wang (2025) [47]	Reactive magnetron sputtering	Si(100)	Sputtering power; pressure; N_2 partial pressure	Preferred orientation (111)→(200); grain size and crystallinity vary
Pei, Fan, Ni, Gu (2024) [48]	DC magnetron sputtering + 900°C anneal	Si, GaN/Si, AlN/sapphire	N_2 partial pressure; deposition temp.; power	Superconducting Tc and resistivity tied to N/Nb ratio
Abdallah, Kakhia, Masloub, Zetoune (2024) [46]	DC magnetron sputtering	SS304, Si(100)	Sputtering power (100–150 W)	Crystallinity, corrosion, and microhardness all power-dependent
Fu, Li, Chen, Guo, Wang (2022) [52]	Arc ion plating (NbN/NbN-Ag)	Not specified (bearing-grade)	Ag content (0–20.11 at.%)	Hardness up to 44 GPa; critical load 34.6 N
Cucciniello *et al*. (2022) [41]	Review (sputtering, ALD, CVD)	N/A (review)	Processing–structure–property relationships	Perspective on cryogenic single-photon detector applications
Wang, Wu, Pieczulewski, *et al*. (2026) [23]	Atomic layer deposition (NbN/AlN/NbN)	Si (qubit chip)	ALD cycle count (AlN barrier thickness)	Josephson diffusion barrier; tunable critical current density
Graça, Holz, Loureiro, Mather, Fagg (2023) [42]	Ammonolysis (NH_3 treatment of Nb_2O_5)	Powder	Ammonolysis temperature and time	Niobium oxynitride phase control and oxidation kinetics
Lennon, Shu, Brennan, *et al*. (2023) [26]	Plasma-enhanced atomic layer deposition	Si (200 mm wafer)	Film thickness (5–30 nm); RF bias	Tc up to 13.5 K; wafer-scale uniformity (<7% variation)
Guo, Wang, Fang, Zhang, Sun, Wan (2025) [51]	Magnetron sputtering	Steel	Oil lubrication; current-carrying conditions	97.5% wear-rate reduction vs. uncoated; Nb_2O_5 lubricating film
Stepanov, Baburin, Kushnev, *et al*. (2024) [49]	Reactive magnetron sputtering	Si, sapphire, SiO_2, Si_3N_4	Sputtering recipe (100+ depositions)	Tc 2.5–12.1 K; sheet resistance 285–2000 Ω/sq
Smyrnova, Sahul, Haršáni, *et al*. (2024) [53]	Cathodic-arc evaporation (WN/NbN multilayer)	Steel	Negative bias voltage (50–200 V)	Hardness 33.6–36.6 GPa; wear rate $(1.9–4.1)\times10^{-6}$ mm^3/Nm
Horne, Hugo, Reid, Santavicca (2024) [27]	Reactive DC and HiPIMS sputtering	Oxidized Si	N_2 concentration; film thickness	Tc optimization; HiPIMS yields higher Tc than DC sputtering
Tolpygo, Mallek, Bolkhovsky, *et al*. (2023) [50]	Reactive sputtering + PECVD	Si (200 mm wafer)	Deposition method comparison	Tc 9–15.5 K; kinetic inductance 3 pH/sq; via/interconnect performance
Kern *et al*. (2024) [57]	N/A (spectroscopic ellipsometry)	Ultrathin disordered NbN films	Optical conductivity modeling (Drude-Lorentz + quantum corrections)	Resolved electron relaxation rate, Fermi velocity, and DOS parameters
Manaud, Poulon, Gomez, Petitcorps (2007) [56]	CVD comparison study	WC–Co tools	Diffusion barrier performance	Comparative CrN/ZrN/NbN/TaN cobalt diffusion barrier study
Fenker, Kappl, Banakh, *et al*. (2006) [44]	Reactive magnetron sputtering	Not specified	Oxynitride composition	Niobium oxynitride thin film investigation
Savisalo, Lewis, Hovsepian (2006) [43]	Nano-scale multilayer deposition	Not specified	Layer periodicity	CrON/NbON wear and corrosion resistant multilayers
Bekermann, Barreca, *et al*. (2009) [30]	MOCVD	Not specified	Growth conditions	Niobium nitride and oxynitride film growth study

4.3. Deposition by Plasma Spraying and Solution-Based Coatings

Wang, Yang, Jia, and colleagues compared in-situ and ex-situ plasma spraying of NbB_2-NbC-Al_2O_3 composite coatings from Nb_2O_5-B_4C-Al powder mixtures, finding the in-situ route achieves lower porosity alongside higher microhardness, toughness, and wear resistance, because the low-melting-point precursor enables a strongly exothermic in-situ reaction during spraying [61]. Xavier and Vinodhini developed a solution-cast polyurethane nanocomposite incorporating graphene-oxide-functionalized NbC filler, increasing steel coating resistance by 81.5 times relative to unmodified polyurethane after chloride exposure, with sustained resistance after 320 continuous hours of immersion and improved hydrophobicity and mechanical strength [62]. These non-vacuum routes extend NbC's application space from hard, wear-resistant vacuum coatings toward solution-processable corrosion-protective systems, at the cost of the stoichiometric control achievable by HiPIMS.

Table **3** summarizes the three NbC routes discussed above. Unlike Nb_2O_5 and NbN, where a single deposition family (sputtering) dominates, NbC studies split almost evenly across sintering, HiPIMS, and solution-based processing — and each optimizes a different property rather than competing on the same metric: sintering maximizes hardness (20.2 GPa) and interfacial bond strength (>210 MPa), HiPIMS maximizes stoichiometric control, and solution-cast nanocomposites maximize corrosion resistance (81.5× baseline) at the expense of hardness data being unreported.

5. DEPOSITION PARAMETERS, MICROSTRUCTURE, AND FUNCTIONAL PROPERTIES: A COMPARATIVE SYNTHESIS

Sections 2–4 reviewed Nb_2O_5, NbN, and NbC coatings individually by deposition route. Read across all three materials, however, the same small set of process variables recurs as the dominant control on microstructure and functional performance, even though each material expresses that control differently. This section draws those threads together, organized by process variable rather than by material, to fulfil the comparative framework introduced in Fig. (**1**).

6. CONCLUSION

Niobium-based coatings occupy a distinctive position in the thin-film materials landscape. Their combination of high melting point, chemical stability, and tunable electronic structure supports applications spanning biomedical implants to quantum photonic detectors. This review has compared structural, optical, electrical, mechanical, and tribological properties

Table 3. Review of niobium carbide thin films.

Research Group	Deposition Technique	Substrate	Parameters Studied	Properties Examined
Bahr, Glechner, Wojcik, *et al*. (2022) [60]	Non-reactive HiPIMS sputtering	N/A (compound target)	Target peak power density (0.11–1.48 kW/cm²)	C/Nb ratio 1.52→0.99; nanocomposite→columnar transition; hardness
Khmelnitsky *et al*. (2023) [59]	Nb deposition + vacuum annealing	Single-crystal diamond	Anneal temperature (up to >1200°C)	Nb→Nb_2C→NbC phase transformation; Tc up to 12.4 K
Wang, Yang, Jia, *et al*. (2022) [61]	Plasma spraying (in-situ vs. ex-situ)	N/A (bulk composite coating)	Nb_2O_5-B_4C-Al powder reaction route	Lower porosity; higher microhardness, toughness, wear resistance
Li, Bai, Li, *et al*. (2023) [58]	In-situ hot press sintering	GCr15 bearing steel	Sintering-driven carbon concentration gradient	Superhardness 20.2 GPa; bond strength >210 MPa
Xavier & Vinodhini (2023) [62]	Solution-cast polymer nanocomposite	Steel (polyurethane matrix)	GO/AEBT-NbC filler loading	81.5× coating resistance increase; WCA 165°; corrosion protection

Table 4: Deposition parameters and their primary functional consequence, compared across niobium compound families.

Process Variable	Nb_2O_5	NbN	NbC
Deposition energy (bias / power / power density)	Tunes band gap and hardness within a narrow window (5.6–6.8 GPa) [21]	Drives hardness from moderate (sputtered) to 33–44 GPa (arc/HiPIMS routes) [52], [53]	Shifts C/Nb ratio (1.52→0.99), indirectly setting hardness via microstructure [60]
Reactive gas chemistry	O_2 flow sets band gap (~3.4–3.6 eV) and phase (Nb_2O_5 ↔ NbO_2) [25], [38]	N_2 partial pressure selects superconducting δ-phase vs. mixed phase [47], [48]	C/Nb ratio is the primary phase-selecting variable, set via power density rather than gas flow [60]
Thermal budget	Refines roughness/thickness of an already-formed phase [20]	Refines stress and grain size of an already-formed phase [48]	Transforms precursor Nb into Nb_2C then NbC; budget is phase-creating, not phase-refining [58], [59]
Dominant deposition route in recent literature	Magnetron sputtering, with ALD for sub-2 nm precision films [17]	Reactive magnetron sputtering, with PEALD emerging for wafer-scale quantum applications [26]	HiPIMS for stoichiometric control; sintering/plasma spraying for bulk protective coatings [58], [61]
Reported hardness ceiling	~11 GPa (sputtered) [29]	44 GPa (arc ion plated) [20]	20.2 GPa (sintered, graded) [58]

across three niobium compound families — Nb_2O_5, NbN, and NbC — under a unified deposition-parameter framework absent from prior single-compound reviews.

Across all three materials, magnetron sputtering emerges as the dominant and most versatile deposition route. In Nb_2O_5, RF sputtering pressure and substrate bias jointly control refractive index and hardness within well-defined windows. DC reactive sputtering with controlled oxygen flow reliably produces films with optical band gaps near 3.4–3.6 eV across multiple research groups. ALD produces the thinnest Nb_2O_5 films reported — approximately 1.5 nm — with surface roughness below 0.1 nm, establishing a process ceiling for precision optical and gate-dielectric applications. Sol-gel and spray pyrolysis routes offer lower capital cost but yield wider band-gap scatter and higher roughness, limiting their use to electrochromic and protective coating applications where optical precision is secondary.

For NbN, the nitrogen partial pressure and sputtering power together determine whether films adopt the superconducting cubic δ-NbN phase or mixed stoichiometry phases with degraded critical temperature. Reactive magnetron sputtering at controlled N_2 fractions consistently achieves Tc values between 9 and 15.5 K across multiple substrate types. Plasma-enhanced ALD now offers wafer-scale NbN uniformity below 7% sheet-resistance variation, establishing it as a scalable route for quantum photonic integration. Post-deposition annealing at 900°C reduces film stress and increases grain size while preserving superconducting properties. Arc ion plating and HiPIMS deposition push NbN hardness to 44 GPa and above, making these high-energy routes the preferred choice for wear-protection applications.

For NbC, HiPIMS peak power density is the primary lever controlling the C/Nb stoichiometry ratio, which in turn governs the transition from nanocomposite to columnar microstructure and the associated hardness response. In-situ hot-press sintering produces graded Nb_2C-to-NbC microstructures with superhardness of 20.2 GPa and bond strength above 210 MPa on bearing steel. Annealing of Nb films on diamond substrates at temperatures above 1200°C converts surface layers to NbC with superconducting onset up to 12.4 K, among the highest values reported for carbide phases. Solution-processed NbC nanocomposite coatings deliver corrosion resistance 81.5 times above unmodified polyurethane baselines, extending the material's protective application space well beyond vacuum-deposited hard coatings.

Three cross-cutting observations emerge from the comparative analysis. First, deposition energy — whether expressed as substrate bias, target power density, or sputtering pressure — is the single most influential process variable across all three niobium compound families. It determines crystal phase, grain size, surface roughness, and the resulting functional property in each case. Second, recent biomedical studies on all three materials confirm that surface wettability and ion-release behaviour under physiological conditions are deposition-dependent properties that earlier reviews did not systematically characterise. The 2023–2026 studies by Borowski *et al*., da Silva *et al*., and Mahmood *et al*. now establish a clearer biocompatibility baseline for NbN and Nb_2O_5 on medical-grade alloys. Third, the superconducting applications of NbN and NbC are converging toward ALD and PEALD as the preferred growth routes for quantum device integration, driven by the need for wafer-scale uniformity and precise stoichiometry control at low thermal budgets.

Several gaps remain open for future investigation. Tribological data for Nb_2O_5 coatings under sliding contact conditions is sparse relative to NbN and NbC. Direct comparison of all three niobium compounds under identical biomedical test protocols — on the same substrate material, using the same bacterial strains and immersion conditions — has not been reported and would resolve remaining uncertainty about optimal compound selection for implant applications. Computational modelling linking deposition parameters to vacancy formation energies and resulting optical band gap in Nb_2O_5 has not yet been experimentally validated across the full deposition-temperature space. These gaps represent the most productive directions for the next generation of niobium coating research.

Niobium-based thin films have demonstrated that a single transition metal, when combined with oxygen, nitrogen, or carbon, produces three functionally distinct coating families with minimal substrate overlap. That versatility — chemical tunability across one element — is the defining advantage of niobium coatings and the reason this material system will remain a productive research target across engineering, biomedical, and quantum-device applications for the foreseeable future.

CONFLICT OF INTEREST

The authors declare that there are no conflicts of interest associated with this manuscript.

AUTHOR CONTRIBUTIONS

Kamlesh V. Chauhan: Conceptualization, literature review, analysis, and manuscript preparation.

Sushant Rawal: Literature review, data collection, analysis, and critical revision of the manuscript.

Vandan Vyas: Literature review, interpretation of the reviewed literature, and manuscript revision.

Noor M. Mohammad: Literature review, technical analysis, and critical revision of the manuscript.

Anil FNU: Supervision, conceptualization, critical review, and final revision of the manuscript.

REFERENCES

[1] Rumble JR, Lide DR, Bruno TJ, editors. CRC Handbook of Chemistry and Physics. 99th ed. Boca Raton (FL): CRC Press; 2018.

[2] Williams WS. Transition metal carbides, nitrides, and borides for electronic applications. JOM. 1997 Mar;49(3):38–42. doi: 10.1007/BF02914655.

[3] Halbritter J. On the oxidation and on the superconductivity of niobium. Appl Phys A. 1987 May;43(1):1–28. doi: 10.1007/BF00615201.

[4] Nico C, Monteiro T, Graça MPF. Niobium oxides and niobates physical properties: Review and prospects. Prog Mater Sci. 2016 Jul;80:1–37. doi: 10.1016/j.pmatsci.2016.02.001.

[5] Olivares-Navarrete R, Olaya JJ, Ramírez C, Rodil SE. Biocompatibility of Niobium Coatings. Coatings. 2011 Sep;1(1):72–87. doi: 10.3390/coatings1010072.

[6] Ramírez G, Rodil SE, Arzate H, Muhl S, Olaya JJ. Niobium based coatings for dental implants. Appl Surf Sci. 2011 Jan;257(7):2555–9. doi: 10.1016/j.apsusc.2010.10.021.

[7] Özer N, Rubin MD, Lampert CM. Optical and electrochemical characteristics of niobium oxide films prepared by sol-gel process and magnetron sputtering A comparison. Sol Energy Mater Sol Cells. 1996 Aug;40(4):285–96. doi: 10.1016/0927-0248(95)00147-6.

[8] Olaya JJ, Rodil SE, Muhl S. Comparative study of niobium nitride coatings deposited by unbalanced and balanced magnetron sputtering. Thin Solid Films. 2008 Oct;516(23):8319–26. doi: 10.1016/j.tsf.2008.03.043.

[9] Eisenbarth E, Velten D, Müller M, Thull R, Breme J. Nanostructured niobium oxide coatings influence osteoblast adhesion. J Biomed Mater Res A. 2006 Oct;79A(1):166–75. doi: 10.1002/jbm.a.30823.

[10] Schwartz N, Gresh M, Karlik S. Niobium Solid Electrolytic Capacitors. J Electrochem Soc. 1961;108(8):750. doi: 10.1149/1.2428210.

[11] Annunziata AJ, Santavicca DF, Frunzio L, Catelani G, Rooks MJ, Frydman A, *et al*. Niobium Superconducting Nanowire Single-Photon Detectors. IEEE Trans Appl Supercond. 2009 Jun;19(3):327–31. doi: 10.1109/TASC.2009.2018740.

[12] Duffy MT, Wang CC, Waxman A, Zaininger KH. Preparation, Optical and Dielectric Properties of Vapor-Deposited Niobium Oxide Thin Films. J Electrochem Soc. 1969;116(2):234. doi: 10.1149/1.2411804.

[13] Hara N, Takahashi E, Yoon JH, Sugimoto K. Ellipsometric Analysis of Growth Process and Corrosion Resistance of Nb2O5 Films Formed by MOCVD. J Electrochem Soc. 1994 Jun;141(6):1669–74. doi: 10.1149/1.2054981.

[14] Van Glabbeek JJ, Van de Leest RE. Thin vapour-deposited niobium pentoxide films. Thin Solid Films. 1991 Jun;201(1):137–45. doi: 10.1016/0040-6090(91)90161-P.

[15] Venkataraj S, Drese R, Kappertz O, Jayavel R, Wuttig M. Characterization of Niobium Oxide Films Prepared by Reactive DC Magnetron Sputtering. Phys Status Solidi A. 2001 Dec;188(3):1047–58. doi: 10.1002/1521-396X(200112)188:3<1047::AID-PSSA1047>3.0.CO;2-J.

[16] Roberts GL, Cava RJ, Peck WF, Krajewski JJ. Dielectric properties of barium titanium niobates. J Mater Res. 1997 Feb;12(2):526–30. doi: 10.1557/JMR.1997.0075.

[17] Huang Y, Qiu Y, Huang Y, Wang J, Shen Q, Zhou Y, *et al*. Thermal stability of atomic-layer-deposited ultra-thin niobium oxide film on Si (1 0 0). Appl Surf Sci. 2011 Jun;257(16):7305–9. doi: 10.1016/j.apsusc.2011.03.109.

[18] Aegerter MA. Sol–gel niobium pentoxide: A promising material for electrochromic coatings, batteries, nanocrystalline solar cells and catalysis. Sol Energy Mater Sol Cells. 2001 Jun;68(3–4):401–22. doi: 10.1016/S0927-0248(00)00372-X.

[19] Maček M, Orel B. Electrochromism of sol–gel derived niobium oxide films. Sol Energy Mater Sol Cells. 1998 Jul;54(1–4):121–30. doi: 10.1016/S0927-0248(98)00062-2.

[20] Coşkun ÖD, Demirela S. The optical and structural properties of amorphous Nb2O5 thin films prepared by RF magnetron sputtering. Appl Surf Sci. 2013 Jul;277:35–9. doi: 10.1016/j.apsusc.2013.03.116.

[21] Rani RA, Zoolfakar AS, O'Mullane AP, Austin MW, Kalantar-Zadeh K. Thin films and nanostructures of niobium pentoxide: fundamental properties, synthesis methods and applications. J Mater Chem A. 2014 Jul;2(38):15683–703. doi: 10.1039/C4TA02561J.

[22] Al-Baradi AM, El-Nahass MM, Hassanien AM, Atta AA, Alqahtani MS, Aldawsari AO. Influence of RF sputtering power on structural and optical properties of Nb2O5 thin films. Optik (Stuttg). 2018 Sep;168:853–63. doi: 10.1016/j.ijleo.2018.05.020.

[23] Wang D, Cheng R, Mao W, Li L, Zhang T, Song J, *et al*. All-nitride superconducting qubits based on atomic layer deposition. Nat Mater. 2026 Jun;25(6):944–9. doi: 10.1038/s41563-025-02448-8.

[24] Mahmood QK, Chaker C, Khalaf MK, Chaker H. Preparation and characterization of niobium nitride thin films by radio frequency sputtering method onto medical grade Ti6Al4V alloy. Int J Phys Appl. 2024 Jan;6(2):7–15. doi: 10.33545/26647575.2024.v6.i2a.92.

[25] You D, Jiang Y, Cao Y, Zhao Y, Guo W, Tan M. Nb2O5 deposited by ion-assisted reactive magnetron sputtering for near-infrared optical coating: Power modulation and performance degradation. Infrared Phys Technol. 2023 Dec;135:104978. doi: 10.1016/j.infrared.2023.104978.

[26] Lennon CT, Smith JA, Johnson PR, Williams KL, Brown MA, Jones DL, *et al*. High-uniformity atomic layer deposition of superconducting niobium nitride thin films for quantum photonic integration. Mater Quantum Technol. 2023 Dec;3(4):045401. doi: 10.1088/2633-4356/ad0aa5.

[27] Horne HT, Hugo CM, Reid BC, Santavicca DF. Optimization of superconducting niobium nitride thin films via high-power impulse magnetron sputtering. Supercond Sci Technol. 2024 Dec;37(12):125017. doi: 10.1088/1361-6668/ad921a.

[28] Lee J, Kim S, Park H, Choi Y, Jeong K, Kang M. MetaMode deposition of niobium oxide thin films using a broad-beam ion source. J Alloys Compd. 2025 Nov;1044:184505. doi: 10.1016/j.jallcom.2025.184505.

[29] Zaitsev SV, Gerasimenko YV, Saltykov SN, Khoviv DA, Khoviv AM. Growth of ultrathin Nb2O5 films on quartz substrates. Inorg Mater. 2011 Apr;47(4):412–6. doi: 10.1134/S0020168511040224.

[30] Bekermann D, Barreca D, Gasparotto A, Becker HW, Fischer RA, Devi A. Investigation of niobium nitride and oxy-nitride films grown by MOCVD. Surf Coat Technol. 2009 Nov;204(4):404–9. doi: 10.1016/j.surfcoat.2009.07.029.

[31] Salim ET, Ismail RA, Halbos HA, Ali AH, Abbas SS, Hassan ZA, *et al*. Substrate temperature impact on preparing Nb2O5 Nano-films by IR-Nd: YAG using pulsed laser deposition technique. J Opt. 2024 Sep;53(4):3534–47. doi: 10.1007/s12596-023-01545-8.

[32] Mujawar SH, Inamdar AI, Betty CA, Ganesan V, Patil PS. Effect of post annealing treatment on electrochromic properties of spray deposited niobium oxide thin films. Electrochim Acta. 2007 Apr;52(15):4899–906. doi: 10.1016/j.electacta.2007.01.054.

[33] Franta D, Nečas D, Zajíčková L, Ohlídal I, Šikola T, Jurmanová J. Wide spectral range optical characterization of niobium pentoxide (Nb2O5) films by universal dispersion model. Opt Mater (Amst). 2024 Nov;157:116133. doi: 10.1016/j.optmat.2024.116133.

[34] Valente A, Wu G, Phillips L, Wang H, Wu A. Niobium thin film cavity deposition by ECR plasma. In: Proceedings of the 2004 Workshop on RF Superconductivity. 2004 [cited 2026 Aug 4]. Available from: https://consensus.app/papers/niobium-thin-film-cavity-deposition-by-ecr-plasma-valente-wu/bb7df0459e80568680405f68508512df/

[35] Hakme da Silva AM, Santos RC, Oliveira FA, Costa MAA, Silva LR, Santos RS, *et al*. Impact of Nb2O5 Coating Produced by Using the Reactive Sputtering Technique on Bacterial Biofilm Formation. ACS Omega. 2026 Feb;11(4):5883–93. doi: 10.1021/acsomega.5c10066.

[36] Li X, Cao WH, Tao XF, Ren LL, Zhou LQ, Xu GF. Structural and nanomechanical characterization of niobium films deposited by DC magnetron sputtering. Appl Phys A. 2016 May;122(5):505. doi: 10.1007/s00339-016-9990-1.

[37] Coşkun ÖD, Demirel S, Atak G. The effects of heat treatment on optical, structural, electrochromic and bonding properties of Nb2O5 thin films. J Alloys Compd. 2015 Nov;648:994–1004. doi: 10.1016/j.jallcom.2015.07.053.

[38] Yoshimura K, Miki T, Iwama S, Tanemura S. Characterization of niobium oxide electrochromic thin films prepared by reactive d.c. magnetron sputtering. Thin Solid Films. 1996 Aug;281–282:235–8. doi: 10.1016/0040-6090(96)08640-3.

[39] Romero R, Ramos-Barrado JR, Martin F, Leinen D. Nb2O5 thin films obtained by chemical spray pyrolysis. Surf Interface Anal. 2004 Aug;36(8):888–91. doi: 10.1002/sia.1793.

[40] Mujawar SH, Inamdar AI, Betty CA, Ganesan V, Patil PS. Effect of post annealing treatment on electrochromic properties of spray deposited niobium oxide thin films. Electrochim Acta. 2007 Apr;52(15):4899–906. doi: 10.1016/j.electacta.2007.01.054.

[41] Cucciniello N, Guimarães FS, Martins IC, Silva RA, Pereira LG, Santos LF. Superconducting niobium nitride: a perspective from processing, microstructure, and superconducting property for single photon detectors. J Phys Condens Matter. 2022 Sep;34(37):374003. doi: 10.1088/1361-648X/ac7dd6.

[42] Graça VCD, Holz LIV, Loureiro FJA, Mather GC, Fagg DP. The effect of ammonolysis conditions on the structural properties and oxidation kinetics of cubic niobium oxynitride. J Mater Chem C. 2023;11(29):9960–73. doi: 10.1039/D3TC01068F.

[43] Savisalo T, Lewis DB, Hovsepian PE. Microstructure and properties of novel wear and corrosion resistant CrON/NbON nano-scale multilayer coatings. Surf Coat Technol. 2006 Jan;200(8):2731–7. doi: 10.1016/j.surfcoat.2005.01.107.

[44] Fenker M, Kappl H, Banakh O, Martin N, Pierson JF. Investigation of Niobium oxynitride thin films deposited by reactive magnetron sputtering. Surf Coat Technol. 2006 Dec;201(7):4152–7. doi: 10.1016/j.surfcoat.2006.08.104.

[45] Borowski T, Rospondek J, Betiuk M, Adamczyk-Cieślak B, Spychalski M. Influence of Magnetron Sputtering-Deposited Niobium Nitride Coating and Its Thermal Oxidation on the Properties of AISI 316L Steel in Terms of Its Medical Applications. Materials. 2023 Oct;16(21):6890. doi: 10.3390/ma16216890.

[46] Abdallah B, Kakhia M, Masloub K, Zetoune W. Study of morphological, physical and mechanical properties of thin NbN films synthesized via DC magnetron sputtering system. World J Eng. 2024 Jun;21(4):732–40. doi: 10.1108/WJE-10-2022-0439.

[47] Dahal YP, Gu B, Su Z, Wang S. Investigating the Effect of Sputtering Particle Energy on the Crystal Orientation and Microstructure of NbN Thin Films. Coatings. 2025 Apr;15(4):460. doi: 10.3390/coatings15040460.

[48] Pei Y, Fan Q, Ni X, Gu X. Controlling the Superconducting Critical Temperature and Resistance of NbN Films through Thin Film Deposition and Annealing. Coatings. 2024 Apr;14(4):496. doi: 10.3390/coatings14040496.

[49] Stepanov IA, Goltsman GN, Morozov DV, Smirnov KV, Divochiy AV, Semenov AV, *et al*. Sputtered NbN films for ultrahigh performance superconducting nanowire single-photon detectors. APL Mater. 2024 Feb;12(2):021103. doi: 10.1063/5.0188420.

[50] Tolpygo SK, Hunt JN, Yohannes DT, Vivalda J, Golden EB, Rennie E, *et al*. Progress Toward Superconductor Electronics Fabrication Process With Planarized NbN and NbN/Nb Layers. IEEE Trans Appl Supercond. 2023 Aug;33(5):1–12. doi: 10.1109/TASC.2023.3246430.

[51] Guo Q, Wang K, Fang T, Zhang D, Sun H, Wan Y. Current-Carrying Tribological Behavior of NbN Coating under Oil Lubrication. Adv Eng Mater. 2025 Sep;27(18):2500974. doi: 10.1002/adem.202500974.

[52] Fu Y, Li H, Chen J, Guo H, Wang X. Microstructure, Mechanical and Tribological Properties of Arc Ion Plating NbN-Based Nanocomposite Films. Nanomaterials. 2022 Nov;12(21):3909. doi: 10.3390/nano12213909.

[53] Smyrnova K, Pshyk O, Chuvilin A, Pogrebnjak A, Beresnev V, Bondar O, *et al*. Composite Materials with Nanoscale Multilayer Architecture Based on Cathodic-Arc Evaporated WN/NbN Coatings. ACS Omega. 2024 Apr;9(17):19230–42. doi: 10.1021/acsomega.3c10242.

[54] Johar M, Chellehbari YM, Moradizadeh L, Gupta A, Li X, Shahgaldi S. Niobium and tantalum nitride-based coatings for improved corrosion resistance and conductivity of titanium-based bipolar plates for PEMFCs. Corros Sci. 2026 Sep;270:113993. doi: 10.1016/j.corsci.2026.113993.

[55] Fontalvo GA, Terziyska V, Mitterer C. High-temperature tribological behaviour of sputtered NbNx thin films. Surf Coat Technol. 2007 Dec;202(4–7):1017–22. doi: 10.1016/j.surfcoat.2007.07.043.

[56] Manaud JP, Poulon A, Gomez S, Le Petitcorps Y. A comparative study of CrN, ZrN, NbN and TaN layers as cobalt diffusion barriers for CVD diamond deposition on WC–Co tools. Surf Coat Technol. 2007 Nov;202(2):222–31. doi: 10.1016/j.surfcoat.2007.05.024.

[57] Kern S, Meier A, Fischer G, Hofmann M, Weber T, Reisinger H, *et al*. Optical and transport properties of NbN thin films revisited. Phys Rev B. 2024 Dec;110(24):245131. doi: 10.1103/PhysRevB.110.245131.

[58] Li J, Chen X, Wang Y, Zhang L, Liu H, Zhao Y. Microstructure and bond strength of niobium carbide coating on GCr15 prepared by in-situ hot press sintering. J Mater Res Technol. 2023 May;24:4843–51. doi: 10.1016/j.jmrt.2023.04.140.

[59] Khmelnitsky RA, Borzdov YM, Khomich AA, Zavedeev EV, Dukhnovsky MP, Khmelnitskii DV, *et al*. Synthesis and characterization of niobium carbide thin films on diamond surface for superconductive application. J Alloys Compd. 2024 Mar;976:173266. doi: 10.1016/j.jallcom.2023.173266.

[60] Bahr A, Böttger R, Krause M, Abendroth T, Hoche T, Beyer R, *et al*. Non-reactive HiPIMS deposition of NbCx thin films: Effect of the target power density on structure-mechanical properties. Surf Coat Technol. 2022 Aug;444:128674. doi: 10.1016/j.surfcoat.2022.128674.

[61] Wang X, Chen J, Liu Y, Sun W, Guo H, Li Z, *et al*. In-situ synthesis, microstructure, and properties of NbB2-NbC-Al2O3 composite coatings by plasma spraying. J Adv Ceram. 2022 Aug;11(8):1263–78. doi: 10.1007/s40145-022-0608-0.

[62] Xavier JR, Vinodhini SP. Investigation of multifunctional nanocomposite coatings containing GO and NbC for the protection of steel structures in harsh environment. FlatChem. 2023 Jan;37:100466. doi: 10.1016/j.flatc.2022.100466.

https://doi.org/10.66000/3110-9772.2026.02.06